Detection and Tracking of Space Objects in Conjunction with Ground and Satellite-Based Sensors

Paul Bernhardt, Sam McKay
Geophysical Institute, University of Alaska, Fairbanks, AK, USA
Bengt Eliasson
Department of Physics, SUPA, University of Strathclyde, Glasgow, UK
W.A. Scales
Electrical and Computer Engineering, Virginia Tech, Blacksburg, VA, USA
Andrew Howarth, Victoria Foss
University of Calgary, Calgary, AB, Canada
Robert 'Lauchie' Scott
Defence R&D Canada Ottawa, Ottawa, ON, Canada

ABSTRACT

New techniques are being developed to track small objects in space using plasma waves produced by orbital debris as they pass through the ionosphere [1, 2, 3]. This process has been studied with computer simulations and laboratory measurements. In situ observations confirming the presence of these plasma waves have been made during space sensor conjunctions with known space objects. Small space objects, when they pass through a structured environment, can also be detected with ground sensors and remote satellite instruments. The HAARP HF facility in Alaska provides this structured environment by generating field aligned irregularities (FAI). Space debris and satellites moving through these irregularities can excite plasma emissions such as whistler, compressional Alfvén, or lower hybrid waves. A whistler wave disturbance is generated by conversion of orbital kinetic energy into an electromagnetic plasma oscillation when a charged space object encounters a FAI [3. 4]. Whistlers propagate undamped at around 9000 km/s from the source regions and can be detected at ranges of several earth-radii. Fast magnetosonic waves have been detected out to ranges of 100 km with in situ electric field probes on the Canadian CASSIOPE/Swarm-E spacecraft. After detection, space debris geolocation is required to update orbit prediction models. In situ measurements from host sensors can provide both range and angle-of-arrival from measurements of electromagnetic (EM) plasma waves in space. The angle of arrive needs a vector sensor of the EM fields to give both the electric (**E**) and magnetic (**H**) vector components of the incident signal from the space debris. Forming the **E** x **B** Poynting flux from the target object, yielding its source direction. A time history of this direction allows estimation of the target trajectory has it passes by the host sensor platform. When charged target debris crosses a field aligned irregularity, it launches a dispersive waveform as a whistler down-chirp or a magnetosonic up-chirp. Propagation from the source point causes temporal dispersion in these signals that stretch in both time and spatial extent. Matched filter processing of the measured signals with wavelet-like, plasma waveforms allows determination of the range to the source at specific generation time.

1. INTRODUCTION

Objects, such as satellites or space debris, may generate plasma waves detectable by another satellite to determine their presence. All satellites in low earth orbit (LEO) pass through the F-Region ionosphere. Ionospheric plasma waves generated by space debris can be used to protect spacecraft from collisional damage. Space debris consists of leftovers from human-made objects – such as discarded launch vehicles or parts of a spacecraft – typically trapped in orbit around the Earth. Currently, NASA tracks over 27,000 such objects in low Earth orbit. The European Space Agency (ESA) estimates that the total mass of all space debris in Earth's orbit is close to 22 million pounds (10 million kilograms). The number of debris that are too small to be tracked, yet large enough to cause severe damage upon impact, is in the millions. Since both space debris and active spacecraft travel at tremendous speeds of about 25,000 kilometers per hour, an impact of even a tiny piece of orbital debris with a spacecraft could create significant issues. Traditionally, space debris are detected with satellite and ground sensors that use optics and ranging radars. These methods, however, cannot detect many smaller debris. Scientists working with the Geophysical Institute at the University of Alaska have shown that space debris produces electric fields that surround them while in motion through the plasma in the ionosphere. Finding space objects with plasma waves, called Space Object identification by in situ Measurements of Orbit-Driven Waves (SOIMOW), relies on creation of plasma oscillations as charged space debris move through space. Both spacecraft and space debris become electrically charged as they are bombarded by solar

photons and electrons from the plasma environment. Hypersonic charged objects can stimulate a wide range of plasma waves as they travel through the ionosphere, crossing the Earth's magnetic field lines.

Space debris is found by flying an electric field sensor on a host satellite through a known field of potential hazards produced by satellite collisions, anti-satellite weapons, explosive rocket booster breakup, etc. An example test of this technique occurred when the Canadian CASSIOPE/Swarm-E satellite pass though the global debris trail left by a major breakup of a Long March 6A (CZ-6A) upper stage associated with the launch of China's Yunai-3 weather satellite. The mass of the upper stage, which is 5800 kg, brokeup at around 05:24 on 12 November 2022. The orbit apogee altitude, perigee altitude, and inclination of the upper stage was 847 km, 813 km, and 98.8 degrees, respectively, at breakup. By the end of January 2023, 533 CZ-6A fragments had been cataloged by the Space Surveillance Network (SSN). on 7 February 2024, the Radio Receiver Instrument (RRI) on CASSIIPE/ Swarm-E collected wave electric field data for 8 minutes from 08:11:30 to 08:19:30 UT as it passed through the CZ-6A debris field. The RRI trajectory (green) is shown in Figure 1 in relation to the CZ-6A breakup objects (pink) and the and the trajectory of the debris object (ID 54606) encountered on 08:15:16 UT at 898 km altitude by the electric field sensor at a minimum range of 2.53 km.

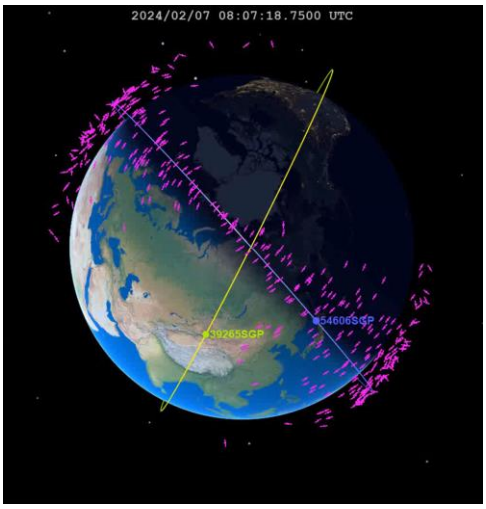

Figure 1. Swarm-E encounters with the Long March CZ-6A debris trail on 7 Feb 2024. During this encounter, the electric field instrument (RRI) was operated at a rapid sampling rate of 62.5 kHz for 8 minutes. The RRI trajectory (green) passed within 2.53 km of one of the CZ-6A fragments (blue) with a radar cross section of 0.04 m^2.

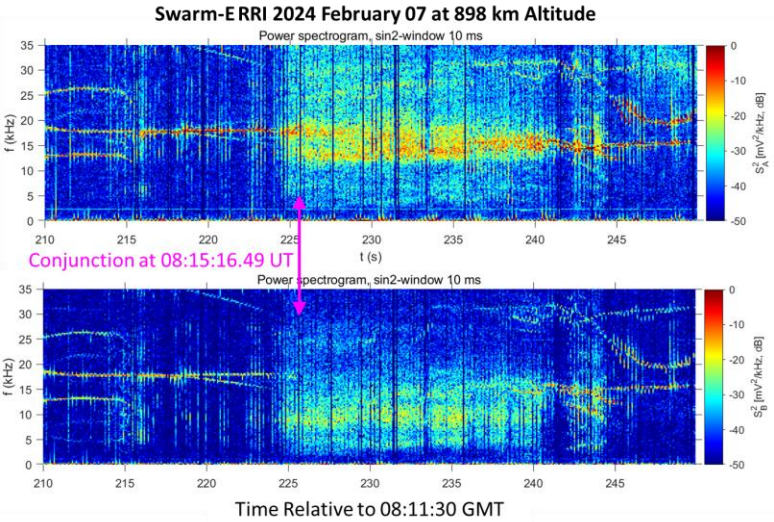

Figure 2. Plasma wave observations with the electric field instrument on Swarm-E made at the closest approach to the CZ-6A debris using the two 5-m dipoles for Channel A (top) and Channel B (bottom). The minimum distance between the target and sensor satellites was 2.54 km at the conjunction time (pink). Enhanced plasma waves are seen primarily below the local lower hybrid frequency of 18.5 kHz in the primarily proton and electron plasma at 898 km altitude.

The plasma wave observations during the close flyby of the RRI to the CZ-6A debris, shown in Figure 2, are typical for the FLASH signature of a space debris passing across magnetic field lines in a plasma as first reported by Bernhardt et al. [1]. The target debris object velocity made an angle nearly perpendicular (93) degrees with the ambient magnetic field vector **B** at a speed of 7.22 km/s. The plasma waves from the space debris are observed after the encounter to a range of 136 km. This unusual behavior in the plasma waves is a clear signature of having detected the space debris. The source and utility of these plasma wave measurements is discussed in the next sections.

2. Space Object Identification with Measurements of Orbit Driven Waves (SOIMOW) Program Elements

Space object generation of plasma waves has been proposed and modeled for over twenty years but actual detection of these waves has only been recently accomplished by the UAF SOIMOW Program. As described in the paper by Bernhardt et al. 2023 [1], both electrostatic and electromagnetic waves have been predicted by a number of authors for excitation with charged space objects moving through the ionosphere. The left column in Figure 1 provides a list of these waves for space objects passing through a uniform plasma. All of the waves and the object itself are difficult to detect because either (1) the plasma disturbance is confined to a magnetic field line (e.g., slow magnetosonic and shear Alfvén waves) or (2) they are electrostatic (e.g., ion acoustic waves and solitons, and lower hybrid waves) so they do not propagate to a significant distance from the source.

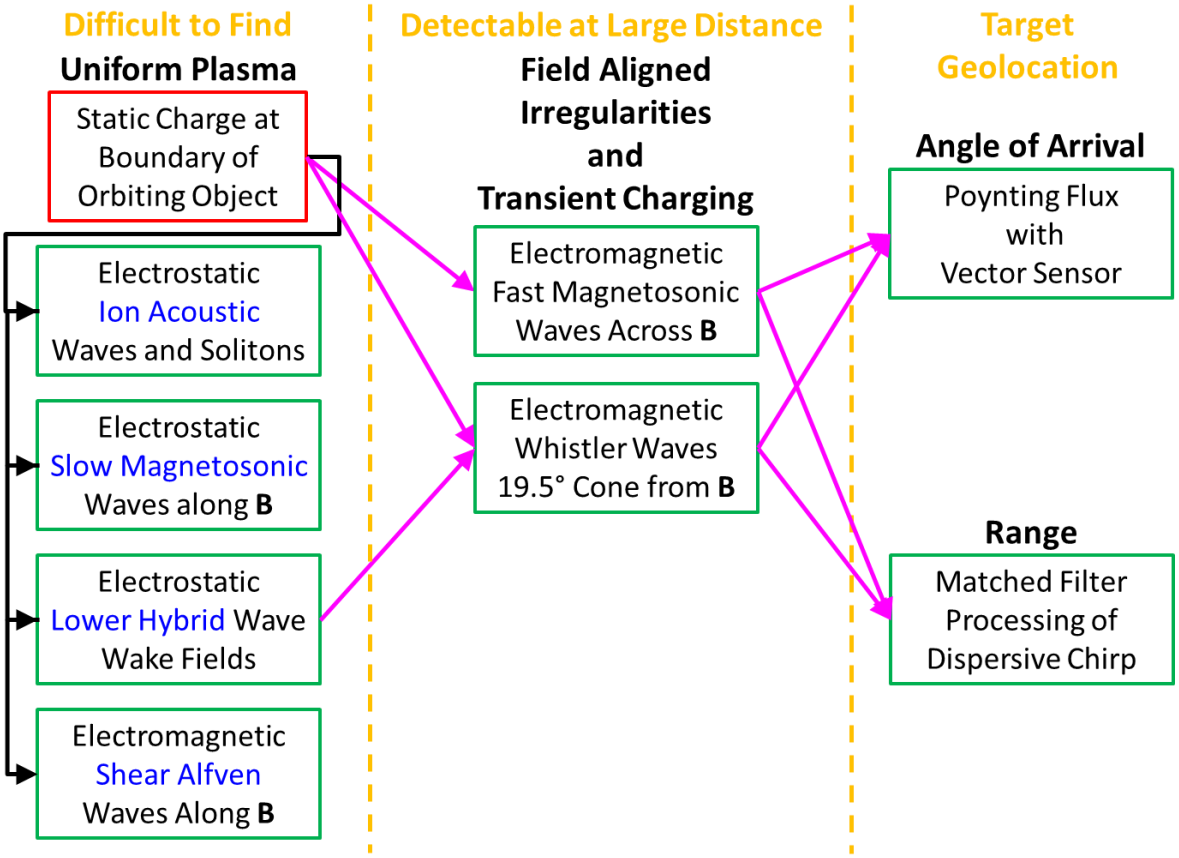

Figure 1. Process for generation of plasma waves from charged objects in hypersonic orbits that yield detectable EM waves suitable for determining positions and predicting the trajectories.

Predictions for waves generated by orbiting space objects include (1) low magnetosonic and electrostatic ion cyclotron, (2) shear Alfvén, electromagnetic ion cyclotron, and ion acoustic, and (3) fast magnetosonic, whistler and electron cyclotron. Both linear disturbances and nonlinear solitons have been postulated in many papers [1]. Detection of space debris by plasma waves in space requires understanding of (1) the process for collection of electric charges on the debris, (2) the generation of waves produced by motion of a charged object in low earth orbit, and (3) remote sensing of the propagating electromagnetic waves or the non-propagating electrostatic waves generated by the moving object.

3. Object Charging Dynamics

Space object charging is key for plasma wave generation for (1) coupling the spacecraft motion to the plasma and (2) launching of electromagnetic plasma waves when there are sudden transients in electric potential (Figure 1). A

model based on spherical symmetry is used to estimate the charges attached to satellites of different sizes. For satellites and space debris propagating through the ionosphere, the ions impact the front (ram) side of the satellite, leading to the ion current [5]

$$I_i = en_0\pi R^2 v_{\rm sat}\,, \tag{1}$$

while the current due to the much faster electrons hitting the satellite from all sides is

$$I_{\rm e} = -en_0\pi R^2\sqrt{\frac{8k_{\rm B}T_{\rm e}}{\pi m_{\rm e}}}\exp\left(\frac{e\phi_0}{k_{\rm B}T_{\rm e}}\right) \tag{2}$$

where the effect of the electron repulsion by the negative potential is considered in the exponential factor for Boltzmann distributed electrons. Setting $I_{\rm i} + I_{\rm e} = 0$ leads to a typical negative floating potential of less than a Volt. However, satellites in polar orbits can acquire a few orders of magnitude higher voltages during intense electron precipitation events [5], leading to a significant increase of the electron current to the satellite compared to Eq. (16) due to the bombardment of the satellite by precipitating electrons. On the other hand, the satellite may also emit photoelectrons due to UV irradiation and become positively charged when sunlit or absorb atmospheric photoelectrons, becoming more negative by a few volts at lower altitudes. Finally, when passing through regions of strong aurora, electron fluxes can dynamically change the charge state of the space object.

For a given satellite potential ϕ_0 relative to the surrounding plasma, the charge state depends on the satellite size and how the plasma forms a sheath around the satellite. In vacuum, a negatively charged sphere of radius R and surface potential ϕ_0 has charges residing on the surface, with the total charge

$$Q = Q_{\rm vac} = C\phi_0 \tag{3}$$

with capacitance $C = 4\pi\epsilon_0 R$. In a stationary plasma, a cloud of opposite charges surrounds the sphere, leading to Debye shielding and rapid decrease of the potential. For a small sphere, $R < \lambda_{\rm De}$ where $\lambda_{\rm De}$ is the electron Debye length (cf. Table 1), the Debye-Hückel potential (for $r > R$) is

$$\phi = \phi_0\frac{R}{r}e^{-(r-R)/\lambda_{\rm De}}. \tag{4}$$

The surface charge, at $r = R$, is then obtained from Gauss' law as

$$Q = Q_{\rm Debye} = 4\pi\epsilon_0\phi_0 R\left(1+\frac{R}{\lambda_{\rm De}}\right) = Q_{\rm vac}\left(1+\frac{R}{\lambda_{De}}\right) \tag{5}$$

Hence, the capacitance is a factor $(1 + R/\lambda_{De})$ larger in plasma compared to the vacuum case due to the Debye sheath of thickness λ_{De}. For a larger sphere, $R > \lambda_{De}$, the sheath thickness depends on the potential and the radius. As an estimate, we use an analytic function fit by *Blackwell et al.* [6] to provide the sheath thickness s, given by

$$s = \left(2.5 - 1.87e^{-0.3R/\lambda_{De}}\right)\left(-\frac{e\phi_0}{k_B T_e}\right)^{2/5}\lambda_{\rm De} \tag{6}$$

which is valid for negative potentials. Using s in place of $\lambda_{\rm De}$ in Eq. (19) gives

$$Q = Q_{\rm sat} = 4\pi\epsilon_0\phi_0 R\left(1+\frac{R}{s}\right) = Q_{\rm vac}\left(1+\frac{R}{s}\right) \tag{7}$$

as an estimate of the charge [7, 8], with values in between the vacuum and plasma Debye sheath charges. Hence, the scaling of the satellite charge with size depends on the radius compared to the Debye length: For macroscopic objects much larger than the Debye length, the charge scales with the surface area $Q \propto R^2$ while for very small objects the scaling is $Q \propto R$. Steady state and time dependent models of this type developed by the University of Strathclyde and Virginia Tech will provide the charging dynamics needed to study plasma wave production by space objects.

Measurements have been made of plasma wave modes generated by the host satellite itself as a result of temporal changes in electric charge potential. The Swarm-E spacecraft (also known as CASSIOPE) was used for these observations. Archived data from the RRI electric field instrument have been analyzed to determine if the orbital motion of Swarm-E satellite body and booms could create plasma emissions. The spacecraft produces a VLF spectral

feature called the Spontaneous Plasma Wave Emission (SPWE). Figure. 2 illustrates an examples of the SPWE near 15 to 20 kHz for satellite motion oblique to the magnetic field $\mathbf{B}_0$. These waves are observed above the local values of the ion cyclotron and lower hybrid frequencies. The data show frequency shifts, spectral spread, and intensity variations that may be related to changes in the object charging, background plasma density, and orbit direction. For the observed SPWE frequency ranges, the SPWE could be local (a) ion acoustic or (b) off-perpendicular lower hybrid waves. The self-generated plasma wave signal seems to intensify as the spacecraft charge becomes less negative. The spacecraft potential is derived from the IRM (Imaging Rapid Ion Mass spectrometer) particle instrument data on Swarm-E by the University of Calgary. Both the RRI and the IRM are part of the e-POP suite of eight instruments. The SPWE is found in a frequency range that can correspond to whistler propagation along the ambient magnetic field **B**. For propagation nearly perpendicular to **B**, these are finite-k_z lower hybrid waves that can be generated which couple to fast magnetosonic waves for remote detection.

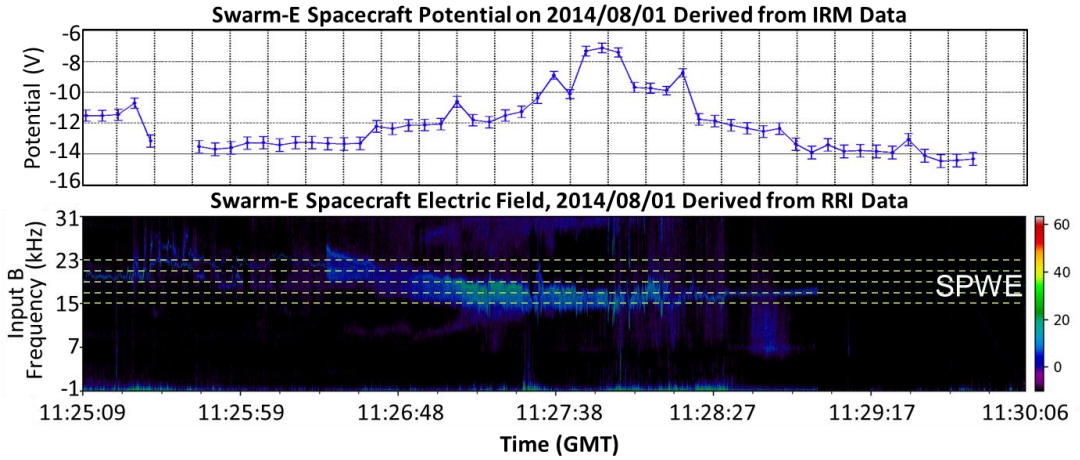

Figure. 2. Satellite plasma wave emission at VLF frequencies correlated with spacecraft charging.

4. Electrostatic Wave Generation

Once the space object becomes charged, passage through a plasma across magnetic field lines can launch electrostatic waves that are confined to with in meters of the object. While difficult to detect locally, these waves can couple to electromagnetic waves that propagate to remote sensors on host satellites. The nonlinear, theoretical model for electrostatic waves such as ion acoustic, slow magnetosonic and lower hybrid waves has been developed at Virginia Tech [9]. The simulations equations for this model are continuity and momentum for fluid electrons,

$$\frac{\partial n_e}{\partial t}+\nabla\bullet(n_e\mathbf{v}_{e\perp})+\cos\theta_B\frac{\partial}{\partial x}n_e\mathrm{v}_{e\|}=\left.\frac{\partial n_e}{\partial t}\right|_{chg},\quad \mathbf{v}_{e\perp}=\frac{(\mathbf{E}+\frac{m_e}{e}\frac{\partial\mathbf{v}_{e\perp}}{\partial t})\times\mathbf{B}_0}{B_0^2},\mathrm{v}_{Te}^2=\frac{\gamma_e\kappa T_e}{m_e},\mathbf{E}=-\nabla\phi$$

$$\frac{\partial\mathrm{v}_{e\|}}{\partial t}=\frac{\cos\theta_B}{B_0}(\frac{\partial\phi}{\partial y}\frac{\partial\mathrm{v}_{e\|}}{\partial x}-\frac{\partial\phi}{\partial x}\frac{\partial\mathrm{v}_{e\|}}{\partial y})-\cos\theta_B(\mathrm{v}_{e\|}\frac{\partial}{\partial x}\mathrm{v}_{e\|}+\mathrm{v}_{Te}^2\frac{1}{n_e}\frac{\partial n_e}{\partial x}+\frac{q_e}{m_e}\frac{\partial\phi}{\partial x})$$

continuity and momentum for fluid ions,

$$\frac{\partial n_i}{\partial t}+\nabla\bullet(n_e\mathbf{v}_i)=\left.\frac{\partial n_e}{\partial t}\right|_{chg}+q,\quad \frac{\partial\mathbf{v}_i}{\partial t}=(\mathbf{v}_i\bullet\nabla)\mathbf{v}_i=\frac{q_i}{m_i}\mathbf{E}+\mathrm{v}_{Ti}^2\frac{\nabla n_i}{n_i}+\nu_{in}\mathbf{v}_i,\mathrm{v}_{Ti}^2=\frac{\gamma_i\kappa T_i}{m_i}$$

particle in cell (PIC) for time dependent charging of the space object,

$$\frac{dx_d(t)}{dt}=\mathrm{v}_d,\frac{dQ_d(t)}{dt}=I_e+I_i,I_e=\pi a^2\sqrt{\frac{8}{\pi}}\mathrm{v}_e\rho_e\exp\frac{e\phi_d}{kT_e},I_i=\pi a^2\sqrt{\frac{8}{\pi}}\sqrt{\mathrm{v}_{Ti}^2+\mathrm{v}_d^2}\rho_i(1-\frac{e\phi_d}{kT_e}),\phi_d=\frac{Q_d(t)}{4\pi\varepsilon_0 a}$$

and Poisson equation for object and wave potentials,

$$\varepsilon_0\nabla^2\phi=-(\rho_e+\rho_i+\rho_d),\rho_e=q_en_e,\rho_i=q_in_i,\rho_d=Q_{dt}F_d(\mathbf{r}-\mathbf{v}_dt),\iiint F_d(\mathbf{r})d^3\mathbf{r}=1$$

with notable features that this system has broad applicability of both ion acoustic waves (red) and inclusion of the polarization drift for lower hybrid waves (blue).

Preliminary results from this set of equations are shown in Figure 3 with the launching of ion plasma oscillations in the wake of a charged space debris moving normal to the magnetic field vector **B**. With motion along the magnetic field, this simulation model would produce ion acoustic solitons predicted in earlier work. This model can produce a variety of phenomena including predicting charging transients and electrostatic waves that drive the propagating EM signals.

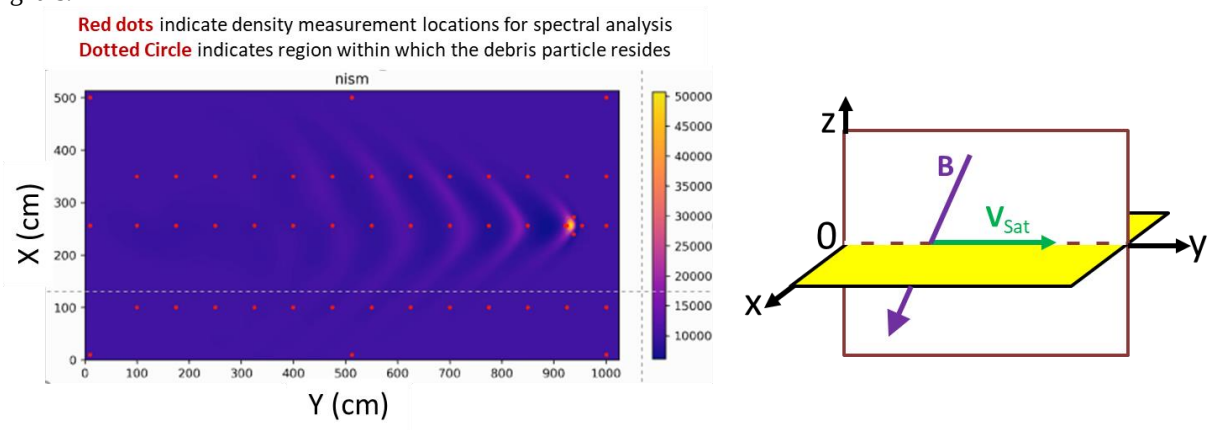

Figure 3. Ion density oscillations associated with ion plasma wave generation from Mach 2 space debris. The simulations are conducted in the yellow plane containing the space object with perpendicularity to the ambient magnetic field direction.

5. Electromagnetic Plasma Wave Generation

The are three ways of launching electromagnetic plasma waves for detection by in situ electric and magnetic field sensors. First, the electrically charged space object can directly excite a shear Alfvén wave that propagates along magnetic field lines. Second, the same object can directly launch whistler or compressional Alfvén waves when crossing a patch of field aligned irregularities (FAIs) or when there is a transient change in its electric potential. Third, electrostatic lower hybrid waves can be converted into whistler waves by crossing FAIs. This process will be investigated using the Electron-Magnetohydrodynamic (e-MHD) and Cerenkov Models described by the SOIMOW authors [1, 3]. During this study effort, the mode conversion of ion acoustic waves into lower hybrid waves or shear Alfvén waves have been examined but is not found to be useful because the limited spatial detectability of these waves.

The SOIMOW program has been selected by the 2024 Basic Plasma Science Facility call for runtime for two consecutive years, starting with the 2024 run year on the UCLA Large Plasma Device (LAPD). These experiments will investigate mode conversion and amplification of whistler waves by lower hybrid waves and will have full support from the BPSF staff in planning and executing the experiments as well as having all existing facility equipment (e.g. antennas, power supplies, diagnostics) is available for use. In addition, the NRL NIKE facility will be used to validate the launching of EM waves with a charged particulates passing through a plasma cloud in a laboratory.

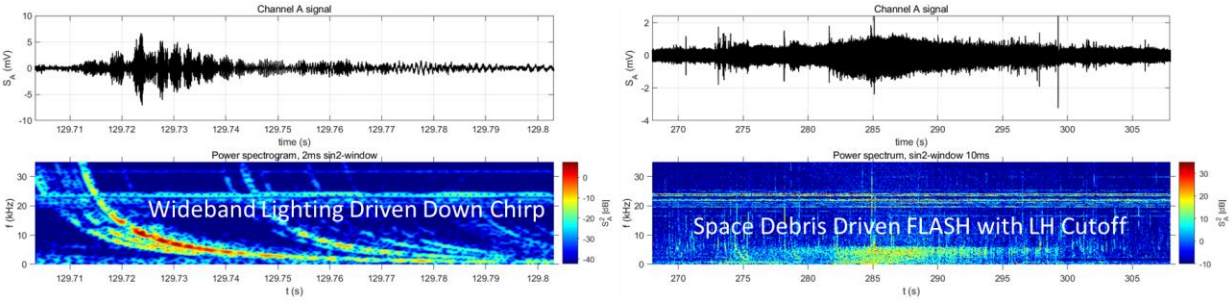

Figure 4. Swarm-E e-POP RRI observations of falling chirp tones from lighting whistlers (left) have a distinct frequency and temporal signature when compared to the band limited spectrum of a space debris (right) for a conjunction with Starlink 2521. The time scale is relative to 03:43:55 on 4 March 2022.

EM wave observations are being made using the radio receiver instrument on Swarm-E plus data from the Japanese ARASE spacecraft. These data are being processed to show detection of space debris. Figure 4 illustrates

a comparison of lightning driven whistlers (left) and satellite generated waves (right) for a satellite encounter with the Starlink 2521 satellite. A conjunction with these objects occurred at 1.17 km range for an altitude of 550 km. The radar cross section of the space debris was 1.17 m^2 but the SOIMOW technique is responding to the charge on the space object which is a function of both the object size and plasma environment.

6. Electromagnetic Plasma Wave Angle of Arrival (AOA)

Detection of space debris, as well as object charge, are obtained with *in situ* plasma wave amplitudes and spectra. The charge is related to the object size using expressions from Sections 3 and 4. Estimates for the location of the object may be obtained from the wave E and H fields using the angle of arrival and range formulas from Table I.

Table I. **Target Properties from Plasma Wave Observations**

Property	Direction of Target Emission	Distance Along B to Plasma Wave Emitter	Distance L Across B to Plasma Wave Emitter
Instrument	Low Frequency Vector Sensor	Plasma Wave Receiver	Plasma Wave Receiver
Measurement	Electric and Magnetic Fields	Plasma Wave Complex Fields	Plasma Wave Complex Fields
Derived Quantity	Poynting Flux Vector	Whistler Frequency	Magnetosonic Wave Frequency
Application Formula	$\langle \mathbf{S} \rangle = \frac{1}{2}\mathrm{Re}(\mathbf{E} \times \mathbf{H}^*)$	$L_{Sat\|\|} = \frac{4\lambda_e \omega_{ce}^{1/2} \omega(t)^{3/2}}{-\partial\omega(t)/\partial t}$	$L_{Sat\perp} = \frac{V_A}{3} \frac{[\omega_{LH}^2 - \omega(t)^2]^{5/2}}{\omega'(t)\omega(t)\omega_{LH}^3}$

Every electromagnetic wave has an electric **E** and magnetic **H** field that is orthogonal to each other and to the direction of travel. The cross product of these fields yields a Poynting Vector away from the source location. This vector can be measured with a vector sensor consisting of 3-axis electric dipole and 3-axis magnetic loop dipole antenna configuration (Figure 5). The accuracy of the AOA measurements will be determined from the vector sensor (VS) antenna pattern or even an interferometer array of satellites of VS's for accurate debris ephemeris. Currently there are no Vector Sensor instruments in low-earth-orbit (LEO) that provide 3-axis data for both the electric and magnetic field vectors in the ELF and VLF (30 Hz to 30 kHz) frequency range. Such a sensor is under development.

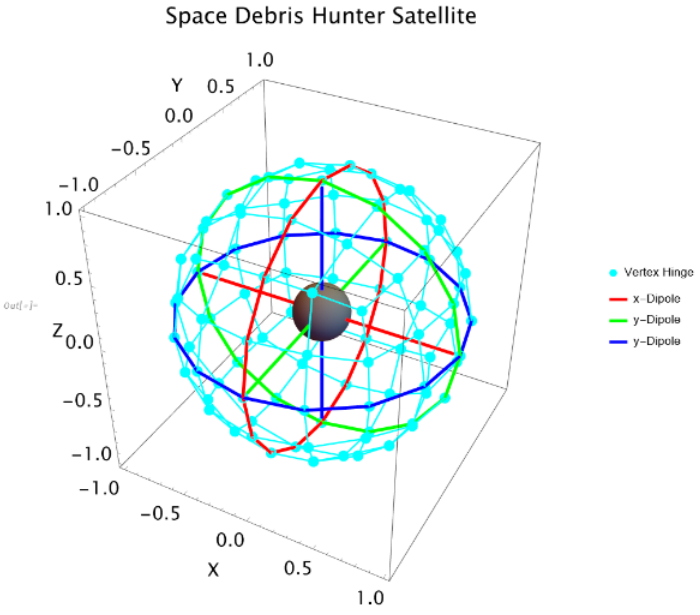

Figure 5. Deployable antenna and central receiver payload to measure the direction of plasma waves produced by space debris.

7. Matched Filter Signal Processing of Plasma Wave Chirps

Each EM plasma wave signal is dispersive, meaning that the frequency components travel at a frequency dependent velocity from the target source to the host receiver. This dispersion provides the basis for determining the range from the host to target. This process is summarized in Figure 6 where the electric field measurements are recorded on a host electric field receiver near space debris passing through a region of field aligned irregularities. Contact with each striation yields a chirp waveform of a down-chip for whistlers and an up-chirp for compressional Alfvén waves. The chirps become stretched in time similar to wavelet waveforms used in spectral analysis. The chirp functions are characterized by a start time (t_0) and a range-to-satellite (L_{ast}). The correlation with the electric field observations is maximized for the target range distance to the generation point at t_0.

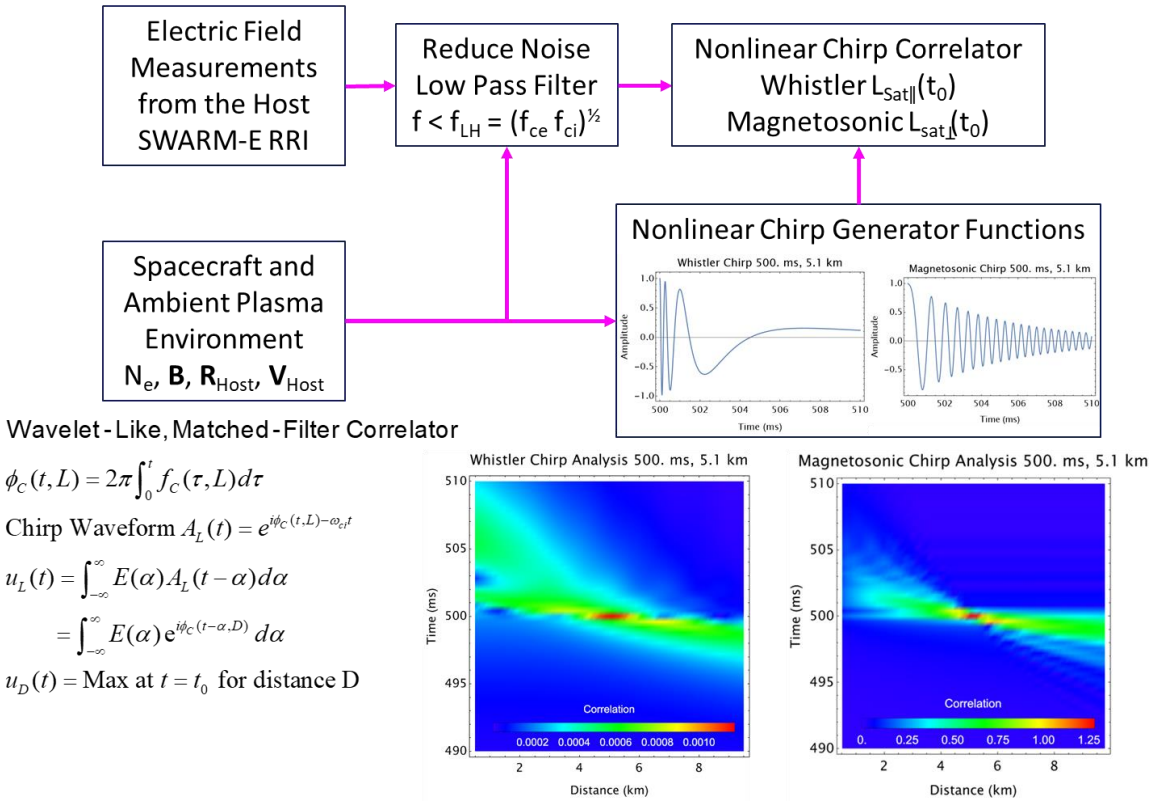

Figure 6. Range signal processing of SOIMOW FLASH events for space debris detection and identification using whistler and fast magnetosonic plasma waves.

Simulations of space objects passing through spatial distributions of plasma density striations will provide representative multi-chirp signals that contain information of positions. Matched filtering of these artificial data will test the range detection algorithms. Data acquired with the RRI instrument on CASSIOPE/Swarm-E will be used demonstrate the utility of this technique. Whistler matched filter processing is applied to the data shown in the left side of Figure 4. The estimated range of the whistler source of ground lighting is found to be about 300 km assuming whistler propagation in a constant ionospheric plasma density. This calculation, which ignores the light-speed propagation from the ground in the 250 km of free space below the ionosphere, gives a reasonable result for a host satellite at 550 km altitude. Whistler and Fast Magnetosonic processing of the data on the right side of Figure 4 has not yet produced definitive results.

This plasma wave process is of interest because it may have an advantage over radar detection of small charged dust particles. The radar detection of the charged particulates seems to require the formation a dusty plasma for dressed particle scatter [10]. The *in situ* SOIMOW process employs enhanced generation of kinetic plasma waves by the streaming of individual dust particles which could also enhance the radar cross [11] as well as exciting EM waves.

Acknowledgment This work at the University of Alaska was supported by IARPA SINTRA Program through the Blue Halo Contract. The European Space Agency's Third Party Mission Program supports the e-POP instruments on the CASSIOPE/Swarm-E satellite.

REFERENCES

[1] P.A. Bernhardt, R.L Scott, A Howarth, G.J. Morales (2023) Observations of Plasma Waves Generated by Charged Space Objects, Phys. Plasmas 30, 092106, https://doi.org/10.1063/5.0155454
[2] R.L. Scott, P.A. Bernhardt, A. Howarth, (2023) Space-based observations of plasma waves during conjunctions between host sensors and space objects, 2023 AMOS Proceedings, Maui, Hawaii.
[3] B. Eliasson and P.A. Bernhardt (2024) The generation of whistler, lower hybrid and magnetosonic waves by satellites passing through ionospheric magnetic field aligned irregularities, Phys. of Plasmas (Submitted).
[4] B. Eliasson, and K. Papadopoulos (2008), Numerical study of mode conversion between lower hybrid and whistler waves on short-scale density striations, J. Geophys. Res.,113, A09315, doi:10.1029/2008JA013261
[5] P.C. Anderson (2012) Characteristics of spacecraft charging in low Earth orbit, J. Geophysical Res. 117, A07308. https://doi.org/10.1029/2011JA016875
[6] D.D. Blackwell, D. N. Walker, S. J. Messer, and W. E. Amatucci (2005) Characteristics of the plasma impedance probe with constant bias, Phys. Plasmas 12, 093510. https://doi.org/10.1063/1.2039627
[7] T G Northrop 1992, Dusty plasmas Phys. Scr. 45 475
[8] Z. Manchester (2010) Measurement and Analysis of the Capacitance of Charged Objects in a Plasma with Applications to Lorentz-Actuated Spacecraft, M.Eng. Report. Cornell University. Ithaca, NY. May, 2010. http://zacmanchester.github.io/docs/Zac_Manchester_MEng_Report
[9] W.A. Scales et al. (1998) Wave generation associated with dust cloud expansion into a plasma Phys. Scr. 238
[10] P.A. Bernhardt, et al. (1995) "Enhanced radar backscatter from space shuttle exhaust in the ionosphere." Journal of Geophysical Research: Space Physics 100.A12: 23811-23818.
[11] M. Rosenberg et al. (1999) Lower hybrid instability driven by charged dust beam, Planetary and Space Science 47, 1517

Debris Tracking Application Quick Look Summary

1. Debris detection from whistler and magnetosonic wave measurements

Charged Space Debris moving through the ionosphere or magnetosphere produces electrostatic lower hybrid waves close to the object. Transient electromagnetic whistler and magnetosonic waves are excited with sudden changes in the charge state of the object or when encountering field aligned irregularities. These waves have been detected out to ranges of 100 km with the electric field sensors on the Radio Receiver instrument.

2. Debris range estimate from whistler and magnetosonic wave measurements

Transient chirp signals are launched from space debris in the ionosphere and magnetosphere. Plasma wave dispersion stretches these signals in both time and space. Matched filter analysis of these signals yields the range to the target debris from the host observation platform. Multiple observations of range versus time provides debris trajectory information.

3. Debris direction of arrival (DOA) from whistler and magnetosonic wave measurements

The electric (E) and magnetic (H) vectors from space debris generated electromagnetic plasma waves can be measured with a vector sensor consisting of three-axis electric dipoles and magnetic loop antennas. The cross product of the electric and magnetic field vectors provides a Poynting vector from the space debris to the sensor platform. The negative of this vector is the direction of arrival that points from the host satellite to the debris object.

4. Debris tracking with simultaneous Plasma Dispersion and Vector Wave Measurements

The time history of range and angle of arrival (AOA) observations along with in situ measurements such as ambient plasma density, background magnetic field, and host spacecraft potential can provide the space debris ephemeris.